

Article type : Research Article

Date Received :28/06/2021

Date Accepted : 22/07/2021

Date published : 01/09/2021



: www.minarjournal.com

<http://dx.doi.org/10.47832/2717-8234.3-3.13>



SPECTROSCOPIC STUDY OF RF MAGNETRON SPUTTERING PLASMA FOR DEPOSITION Ti6Al4V THIN FILM

Dawood S. ALI¹ & Omar M. DAWOOD²

Abstract

In this work, RF magnetron sputtering plasma for the deposition of Ti6Al4V thin film has been investigated by using optical emission spectroscopy at argon working pressure of 5×10^{-3} mbar. The emission lines intensity of the plasma were measured using a spectrometer, and the identify peaks within the selective range of patterns and matched with the standard data from the NIST website to measure the plasma parameters. Since the sputtering power plays an important role to the growth of thin film, so the effect of sputtering power of 50, 75, 100, 125 and 150Watt has been studied on produced plasma parameters. The size of Ti6Al4V sputtering target was 50mm in diameter. The argon gas flow was 40 s ccm. One can observe that the lines intensities increased with increasing the sputtering power. The plasma temperature increases from 1.86 to 2.15 eV, while its density increased from 2.69×10^{18} to 2.94×10^{18} cm⁻³ with increasing the rf power from 50 to 150 W, which effect on sputtering rate.

Keywords: Optical Emission Spectroscopy; Rf Magnetron Sputtering; Thin Films.

¹ General Directorate of Education in Anbar, Iraq, dawoodsalman2020@gmail.com, <https://orcid.org/0000-0002-3963-177X>

² Anbar University, Iraq, esp.omarm.dawood@uonbar.edu.iq, <https://orcid.org/0000-0001-5934-9125>

Introduction

Radio frequency (rf) plasma is commonly used as a deposition or surface treatment technique using low temperature plasma in many industries such as the electronics industry[1], aerospace[2], and biology[3]. Rf plasma contains ions with high energy and reactive species, that are widely applied in the surface etching and deposition of thin-film semiconductors. Although rf plasma has been used on an experimental basis, its diagnosis is important in order to establish a relationship between the properties of the plasma and the final product and to better understand the technique for use in different conditions to obtain the desired product [4]. The Penning discharge was a first stage to the building of a magnetron[5]. The development of magnetron sputtering with new designs allowed the deposition process at higher rates [6], To manufacture high purity semiconductors or to make high quality films for optical applications. In comparison with other physical deposition methods, the magnetron sputtering technique has advantages, the most important of which is that the atoms possess additional kinetic energy, which leads to the deposition of more coherent films with uniform coverage. It can also be used in the formation of many compounds thin films of different proportions at a much lower temperature, as the excess heat may affect temperature sensitive substrates [7]. Magnetron sputtering differs from the traditional discharge sputtering method by adding magnets behind the cathode to generate magnetic fields that focus the plasma in a narrow spot on the target, which increases the sputtering process. At present, the magnetron sputtering method is widely used for depositing nano-structured films and superconducting materials thin films [8]. By changing the shape of the magnetron used, it can increase the sputtering efficiency and the quality of the deposited films. The electrons and ions of high energy that hit the thin film during preparation also contribute to changing their properties and their crystal structure [9]. During plasma deposition process, the required plasma parameters such as plasma temperature and plasma density should be determined and their dependence on electrical discharge parameters such as applied voltage and operating pressure understood. There are several methods for plasma diagnosis, such as spectroscopy, Langmuir probe and microwave interference. etc. Optical methods of plasma diagnostics are an important technique for examining several parts of a plasma without changing their state [10]. The optical emission spectroscopy is one of these techniques, which is analysis depends for the light plasma emission from species, such as atoms and ions, resulting from the interaction of electrons with these species, which in turn reveals the plasma properties. Four plasma models were suggested, according to electron interaction, by MC Whiter criterion. There are several methods for calculating the mean plasma temperature from the emission spectrum. The easiest one is the intensity ratio between two lines[11], which has been used in this study for two argon lines emitted from the rf discharge of argon gas.

The intensity of the spectral lines depends on the electron temperature (kTe), and also depends on the intensity of the density of excited states. Therefore, (kTe) can be calculated from the ratio between the intensities of the spectral lines using the Boltzmann plot relation[12]:

$$kT_e = (E_2 - E_1) \left[\ln \frac{I_1 \lambda_1 g_2 A_2}{I_2 \lambda_2 g_1 A_1} \right]^{-1} \quad (1)$$

The indices 1 and 2 denotesto the two used lines, I is the intensity, k is the Boltzmann constant, g is the statistical weight, E is the excited state's energy and A is the probability of transition. The electron concentration (ne)The density of electrons can be calculated from the ratio between the strengths of the atomic and ionic lines using the Boltzmann-Saha equation [14]:

$$n_e = \left(\frac{2\pi m_e K}{h^3} \right)^{3/2} \times \left(\frac{2A_2 g_2 \lambda_1 I_2}{A_1 g_1 \lambda_2 I_1} \right) e^{\frac{-E_2 - E_1}{T_{ex}}} \times (T_e)^{3/2} \quad (2)$$

Here 1 and 2 refer to the atomic and ionic lines respectively, E1 is the energy of the excited levels, E2 is the plane energy of the neutral atoms and ΔE is the lowest ionization energy.

2. Material Methods

Figure 1. Shows a schematic diagram of the parts of the RF sputtering system that used in this work. The vacuum chamber was made of stainless steel. The length of the chamber is 20 cm, and height of 50 cm. Pure argon gas(99.9% impurity) was used as a working gas. The distance between the cathode and the anode electrodes is 10 cm. Different RF sputtering power were applied from 50, 75, 100, 125 and 150 Watt to produced discharge. Spectrum measurements were recorded by using the spectrometer model VS2100. The emitted lines argon are measuredwithin the range of 200-900 nm and kTe is measure using the spectral lines Ar I (750.296 nm) and Ar II

(434.052 nm) were identical with the Atomic spectra database (NIST) [13]. The collimated lens put near the cathode electrode, i.e. in an area negative glow discharge region (NG), as shown in Figure1.

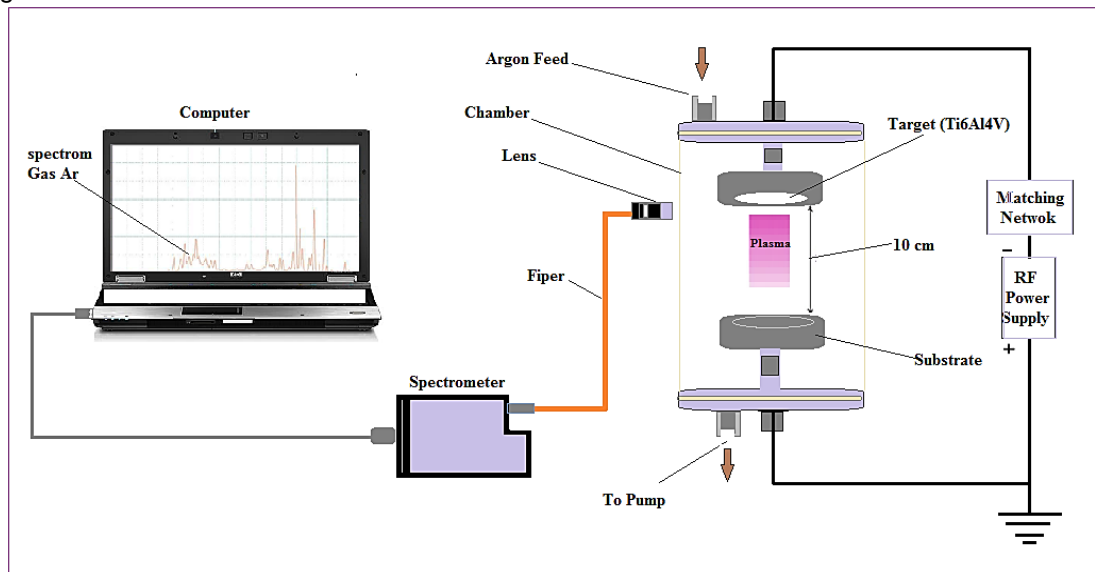


Figure1. The schematic of rf magnetron sputtering setup.

3. Results and Discussion

The spectral emission of argon produced from discharge at different RF power, from 50 to 150 Watt, were shown in Figure 2. The spectra show many peaks corresponding to atomic and ionic emissions (ArI and ArII), in addition to weak peaks corresponding to the metals Al, Ti and V that sputtered into the chamber, as illustrated in expanded figure (Fig. 2-b). The metals peaks have small intensities comparing with argon peaks as due to the low contents of sputtered metal atoms and ions in gas phase comparing with Ar gas content. The lines intensity of ArI (750.296 nm) and ArII (434.052 nm) were matched with the data from National Institute of Standards and Technology (NIST), and used to measure KTe using equation (1). The parameters of the specified lines are taken from the (NIST), including the upper and lower levels energies, statistical weights multiply the probabilities of transition (gA), as shown in Table 1.

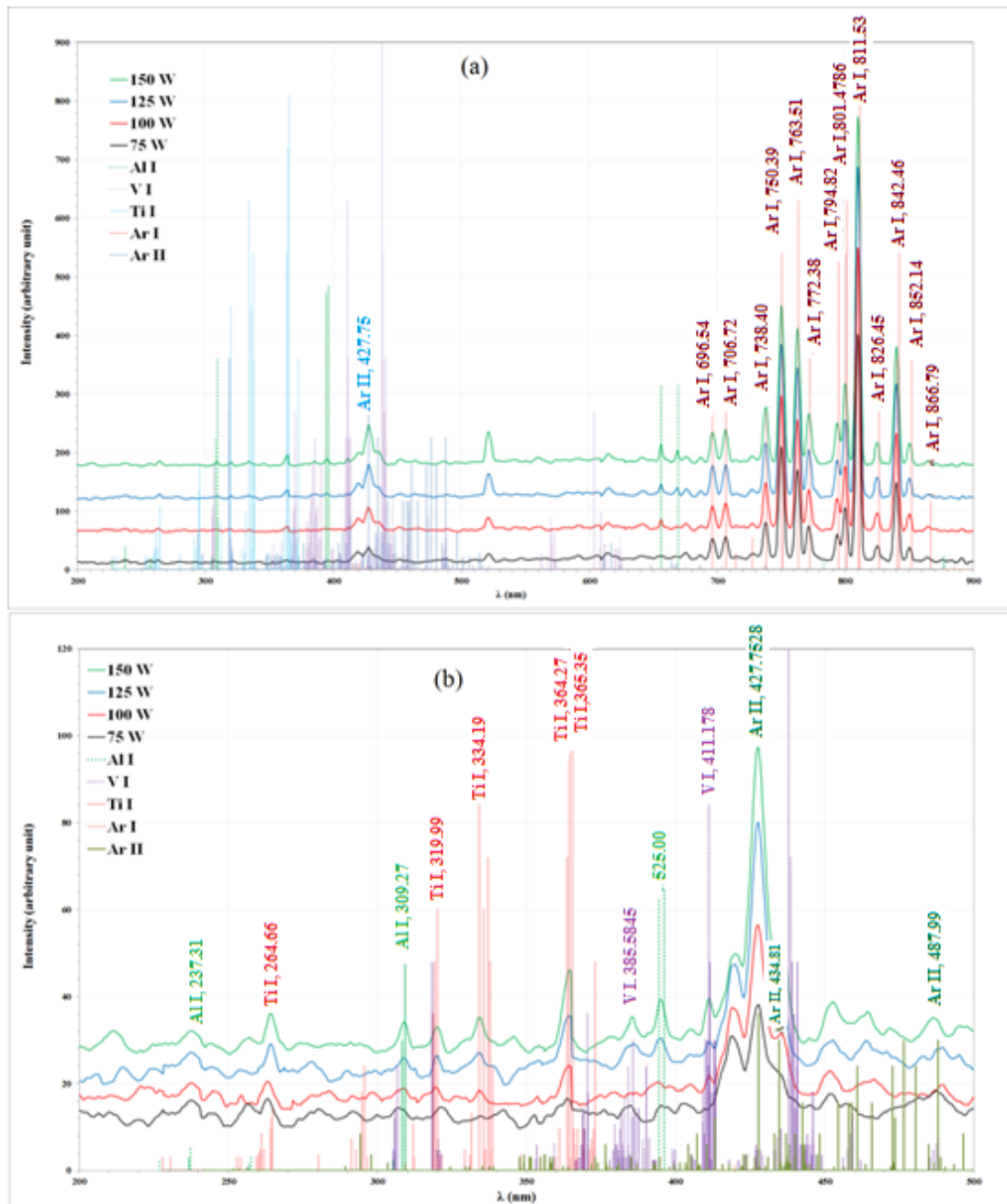


Figure 2. Emission spectra attained by spectroscopy for wavelength range 200 – 900 nm (a) and 200- 500 nm (b).

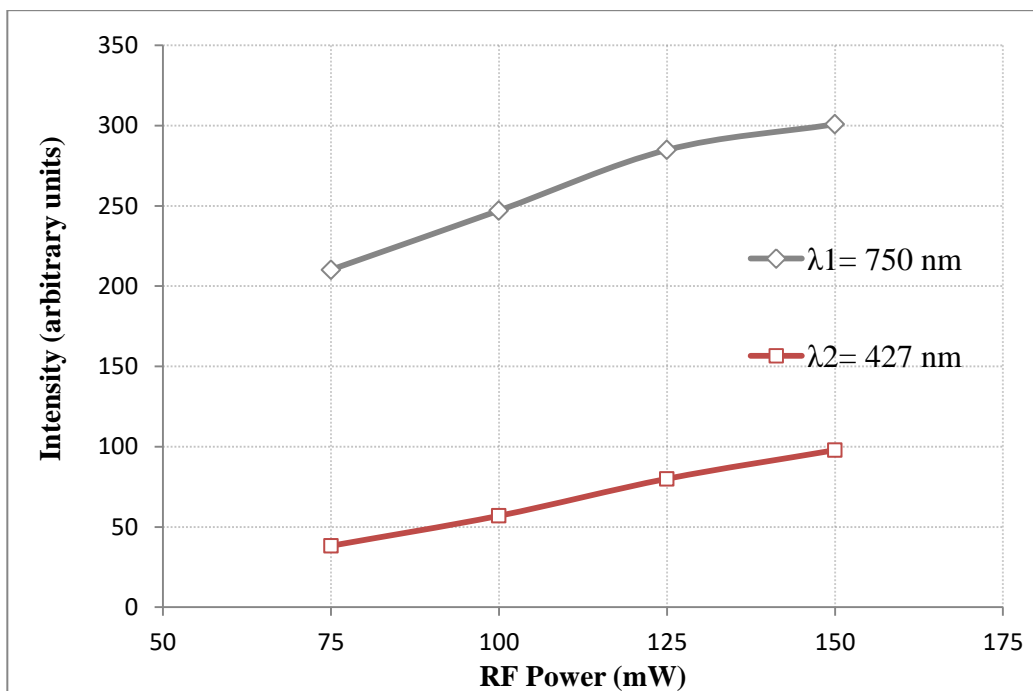
Table 1. Wavelength statistical weight multiply transition probability, Energy levels of the two lines used to calculate Te[13].

Wavelength (nm)		Statistical weight. Transition probability		Upper level energy (eV)	
ArI	ArII	g1A1	g2A2	E1	E2
750.296	427.75	4.45×10^7	3.2×10^8	13.47988	21.35180

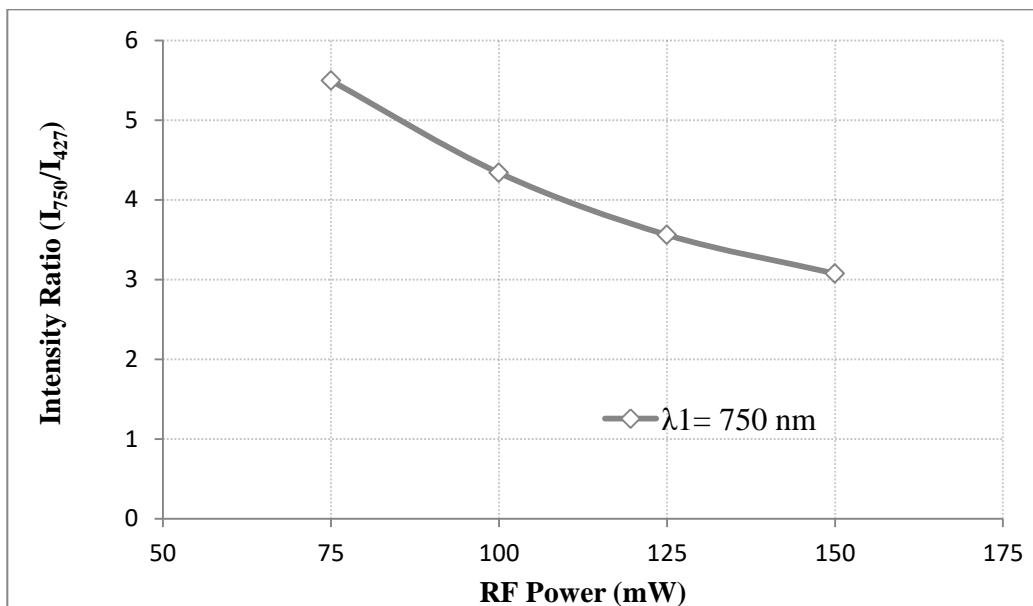
Figures 3 represent the difference of lines intensity for 750.39 nm lines and 427.75 nm lines for ArI and ArII respectively against the rf power.

The intensities for the ArI and ArII increase with the increasing rf power due to increasing electrons energy which leads to increase excitation properties for both species but with different

increment ratio, due to the variation in their excitation cross section at same energy [13]. These results are in agreement with results of reference[15].



Figurer 3. Variation of (750.39 and 427.75nm) lines intensity with RF power at 5×10^{-3} mbar.



Figurer 4. Variation of intensity ratio of (750.39 to 427.75nm) lines with RF power at 5×10^{-3} mbar.

Figure 5 displays the peaks profile and their Lorentzian fitting for the 763 nm line to find the line width $\Delta\lambda$ for the different RF power. The result indicates that the width increases with increasing RF power indicating on increasing the electron density according to Stark broadening effect.

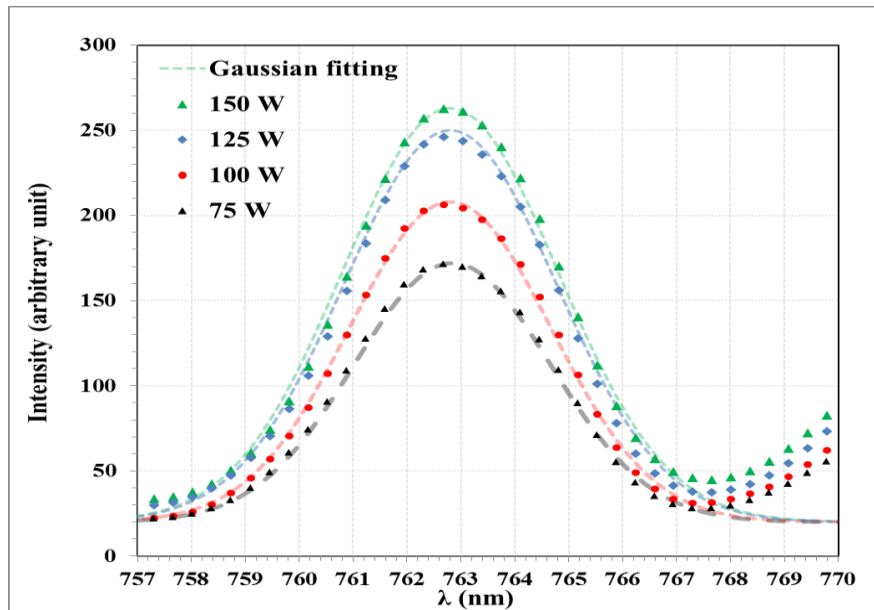


Figure 5. Lorentzian fitting for the 763 nm Ar line at different rf powers.

Figure 6 shows the variation of electron temperature T_e and electron density (n_e) with RF power. The result illustrates that both T_e and n_e increase with growing rf power. This result can be explained by remarking that the emitted electrons from the powered electrode surface perform significant roles in ionization and excitation processes. Thus, with increasing RF power, the secondary electrons that emitted from the electrodes will become more energetic with increasing of rf power and of course which indicated T_e [15]. The plasma density increases with increasing of rf power due to the increasing the ionization process probability with increasing electrons energy.

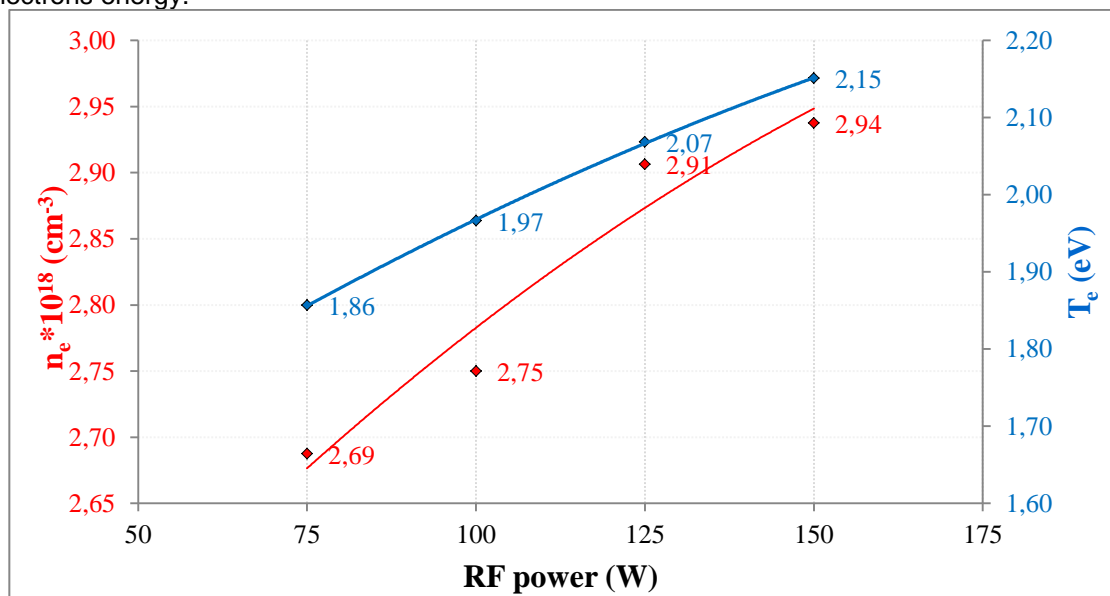


Figure 6. Variation of T_e and n_e with the rf power.

Figure 7. illustrates the X-ray diffraction analysis of prepared Ti6Al4V thin films shows different power (50, 75, 100, 125 and 150) W glass slides. XRD curves show that the (Ti6Al4V) films have a polycrystalline structure with peaks located at ($2\theta \approx 38^\circ$ and 53°) belong (110) and (102) direction identify with standard no. 96-900-8518 for hexagonal Ti. It is note that increases the RF power, leads to increase peaks intensity (i.e. increase films crystallinity). This might be due to increasing the ablated material hence increase film thickness or due to enhancement of films crystallinity due

to increasing energy that delivered to the thin film cause to merge the adjacent particles by removing the grain boundaries. This process cause to increase the average crystallite size which effect on thin properties of the prepared samples. A significant reduce of line broadening indicate the increasing of crystallite size [16, 17].

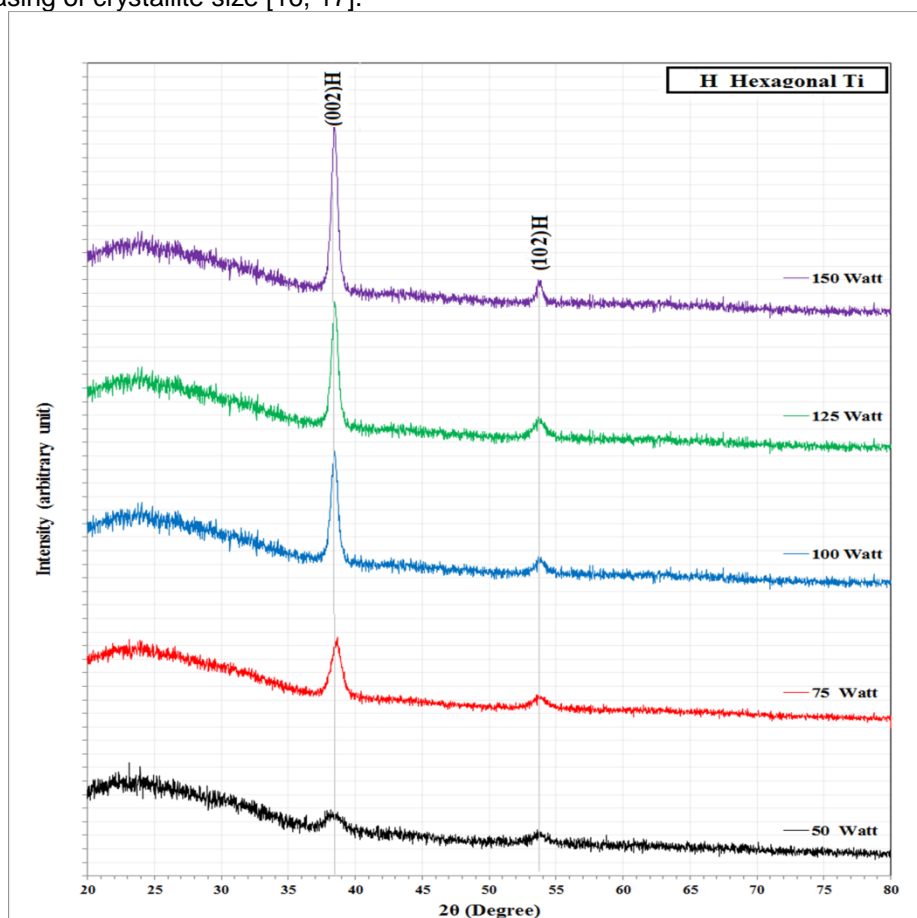


Figure 7. XRD patterns of (Ti6Al4V) films prepared on glass slides at different sputtering power.

4. Conclusions

In this work the effect of rf power, during Ti6Al4V thin film deposition, on the plasma parameters were investigated in more details. The optical spectrometer device was used as plasma of the rf discharge. The results shown that the increasing of the applied power cause to increase of emission intensities. As well as, the results showed that both the plasma density and temperature slowly increased with the increment of the rf power.

References

- Z. J. Radzinski, "Optical emission spectroscopy of high density metal plasma formed during magnetron sputtering," *J. Vac. Sci. Technol. B Microelectron. Nanom. Struct.*, vol. 15, no. 2, p. 202, 1997.
- A. M. Daltrini, S. A. Moshkalev, L. Swart, and P. B. Verdonck, "Plasma parameters obtained with planar probe and optical emission spectroscopy," *J. Integr. Circuits Syst.*, vol. 2, no. 2, pp. 67–73, 2007.
- A. Fridman, *Plasma Chemistry*. New York: Cambridge University Press, 2008.
- A. Dyson, P. Bryant, and J. E. Allen, "Multiple harmonic compensation of Langmuir probes in rf discharges," *Meas. Sci. Technol.*, vol. 11, pp. 554–559, 2000.
- E. Nasser, *Fundamentals of gaseous ionization and plasma electronics*. John Wiley & Sons, Inc., 1971.
- J. G. J.A Thornton, "Sputter deposition processes," *Handb. Depos. Technol. Film. Coatings*, pp. 275–337, 1994.
- N. Li, J. P. Allain, and D. N. Ruzic, "Enhancement of aluminum oxide physical vapor deposition with secondary plasma," *Surf. Coat. Technol.*, vol. 149, no. 161, 2002.

- A. S. Hasaani, "Magnetic Field Effect on the Characteristics of Large-Volume Glow Discharge in Argon at Low Pressure," *Iraqi J. Sci.*, vol. 57, pp. 135–144, 2016.
- R. Tang et al., Breakdown and Ignition Limits in LaB6 Hollow Cathode Discharges, vol. 29, no. 9. 2013.
- A. A. Garamoon, A. Samir, F. F. Elakshar, A. Nosair, and E. F. Kotp, "Spectroscopic study of Argon DC glow discharge," *IEEE Trans. Plasma Sci.*, vol. 35, no. 1, pp. 1–6, 2007.
- F. U. Khan, N. U. Rehman, S. Naseer, M. A. Naveed, A. Qayyum, N. Khattak, and M. Zakauallah, "Diagnostic of 13.56 MHz RF sustained Ar – N2 plasma by optical," *Eur. Phys. J. Appl. Phys*, vol. 45, p. 11002, 2009.
- H. Park, S. J. You, and W. Choe, "Correlation between excitation temperature and electron temperature with two groups of electron energy distributions," *Phys. Plasmas*, vol. 17, no. 10, pp. 1–4, 2010.
- "NIST Atomic Spectra Database." [Online]. Available: <http://kinetics.nist.gov/index.php>.
- M. Umranshan, Principles of Plasma Physics for Engineers and Scientists. New York, 2011.
- N. D. M. A. Hassouba, "A Comparative Spectroscopic Study on Emission Characteristics of DC and RF Discharges Plasma using Different Gases.," *Life Sci. J.*, vol. 11, no. 9, pp. 656–666, 2014.
- R. Filip, "Alloying of surface layer of the Ti-6Al-4V titanium alloy through the laser treatment," *J. Achiev. Mater. Manuf. Eng.*, Vol. 15, No. 1, pp. 174–180, 2006.
- C. M. Garzón, J. E. Alfonso, and E. C. Corredor, "Characterization of adherence for Ti6Al4V films RF magnetron sputter grown on stainless steels," *Dyna*, Vol. 81, No. 185, pp. 175–181, 2014.